

# Highly Miniaturized On-Chip 180° Hybrid Employing Periodic Ground Strip Structure for Application to Silicon RFIC

Young Yun

**A highly miniaturized on-chip 180° hybrid employing periodic ground strip structure (PGSS) was realized on a silicon radio frequency integrated circuit. The PGSS was placed at the interface between SiO<sub>2</sub> film and silicon substrate, and it was electrically connected to top-side ground planes through the contacts. Owing to the short wavelength characteristic of the transmission line employing the PGSS, the on-chip 180° hybrid was highly miniaturized. Concretely, the on-chip 180° hybrid exhibited good radio frequency performances from 37 GHz to 55 GHz, and it was 0.325 mm<sup>2</sup>, which is 19.3% of a conventional 180° hybrid. The miniaturization technique proposed in this work can be also used in other fields including compound semiconducting devices, such as high electron mobility transistors, diamond field effect transistors, and light emitting diodes.**

**Keywords: 180° hybrid, periodic ground strip structure (PGSS), radio frequency integrated circuit (RFIC), coplanar waveguide, diamond.**

---

Manuscript received Mar.15, 2010; revised June 27, 2010; accepted July 26, 2010.

This research was supported by Basic Science Research Program through the National Research Foundation of Korea (NRF) funded by the Ministry of Education, Science and Technology (2010-0007452). This work was financially supported by the Ministry of Knowledge Economy (MKE) and the Korea Industrial Technology Foundation (KOTEF) through the Human Resource Training Project for Strategic Technology. This work was also partly supported by the Grant of the Korean Ministry of Education, Science and Technology (The Regional Core Research Program/Institute of Logistics Information Technology).

Young Yun (phone: +82 51 410 4426, email: yunyoung@hhu.ac.kr) is with the Department of Radio Communication Engineering, Korea Maritime University, Busan, Rep. of Korea.  
doi:10.4218/etrij.11.0110.0146

## I. Introduction

180°/90° hybrid couplers and dividers [1], [2] are required for signal division/coupling in power amplifiers [3], balanced amplifiers, and balanced mixers [4]. A development of highly miniaturized on-chip couplers is indispensable for application to silicon radio frequency integrated circuit (RFIC). Especially, with an evolution of silicon CMOS device process technology, highly integrated silicon integrated circuits (ICs) including radio frequency (RF) and base-band block have been developed [5]. However, hybrid coupler/dividers are fabricated outside of ICs due to their large sizes, which have been an obstacle to a realization of a fully-integrated silicon front-end.

In this work, to solve the above problem, a highly miniaturized on-chip 180° hybrid employing periodic ground strip structure (PGSS) was realized on silicon RFICs.

## II. Highly Miniaturized On-Chip 180° Hybrid Employing PGSS on Silicon Substrate

Transmission lines employing periodic structures have been fabricated on compound semiconducting substrates [6], [7] and silicon substrates [8], [9]. They showed slow-wave characteristics, and they were suitable for application to miniaturized passive components. In this work, a transmission line employing PGSS [9] was used on an application for a miniaturized on-chip 180° hybrid on a silicon substrate.

Figure 1 shows the on-chip 180° hybrid employing PGSS on a silicon substrate. As shown in Fig. 1, the 180° hybrid consists

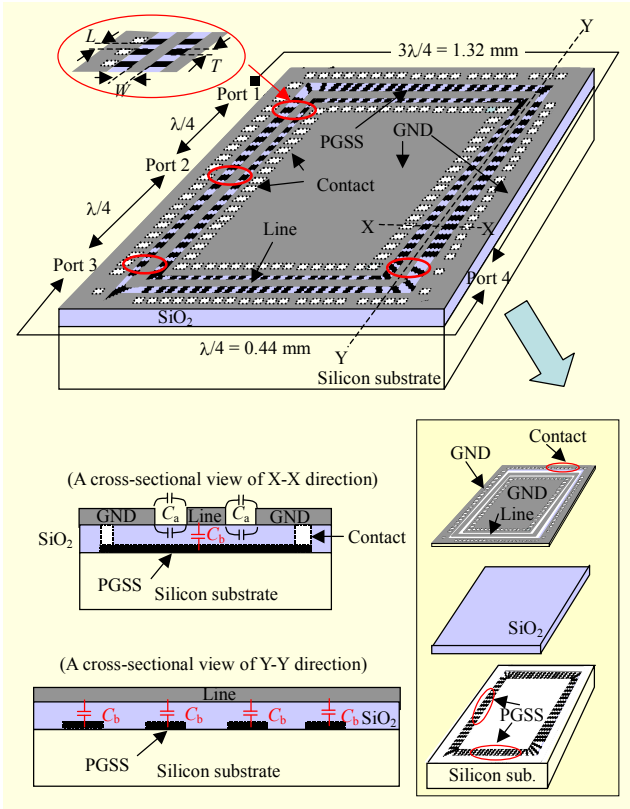


Fig. 1. Structure of on-chip 180° hybrid employing PGSS on silicon substrate.

of four section transmission lines: three transmission lines with a length of  $\lambda/4$  and one transmission line with a length of  $3\lambda/4$ . Each transmission line was realized using coplanar waveguides employing PGSS. Although a conventional 180° hybrid occupies a very large area on an RF circuit [1], the size of the 180° hybrid employing PGSS was highly reduced due to a short wavelength characteristic of the coplanar waveguide employing PGSS. The reason for the size reduction of the 180° hybrid employing PGSS can be explained as follows. As shown in this figure, PGSS exists at the interface between SiO<sub>2</sub> film and silicon substrate, and it was electrically connected to top-side ground planes (GND planes) through the contacts. Therefore, PGSS was grounded through GND planes. As is well known, a conventional coplanar waveguide without PGSS has only a periodical capacitance  $C_a$  ( $C_a$  is shown in Fig. 1) per a unit length, while a coplanar waveguide employing PGSS has additional capacitance  $C_b$  as well as  $C_a$ . As shown in Fig. 1,  $C_b$  is a capacitance between a line and PGSS. In other words, a total capacitance (per unit length) of the coplanar waveguide employing PGSS corresponds to  $C_a + C_b$ , but, a total capacitance of a conventional coplanar waveguide without PGSS corresponds to  $C_a$ . Therefore, the coplanar waveguide employing PGSS exhibits wavelength ( $\lambda_g$ ) much shorter than conventional coplanar waveguide, because

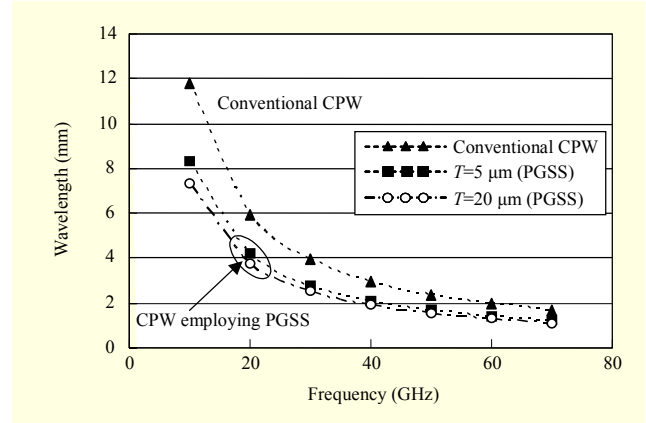


Fig. 2. Measured wavelength of coplanar waveguide employing PGSS and conventional one.

$\lambda_g$  is inversely proportional to the periodical capacitance, in other words,  $\lambda_g = 1/[f(LC)^{0.5}]$ .

Figure 2 shows the measured wavelength of a coplanar waveguide employing PGSS and a conventional coplanar waveguide. The wavelength was obtained from the measured phase of insertion loss  $S_{21}$  by using

$$\lambda = \frac{-2\pi l}{\angle S_{21}}. \quad (1)$$

In (1),  $\lambda$ ,  $\angle S_{21}$ , and  $l$  are the wavelength, measured phase of the insertion loss  $S_{21}$ , and physical length of transmission line, respectively. The coplanar waveguides were fabricated on a silicon substrate with a height of 600  $\mu\text{m}$ . The distance between ground strip  $L$  and line width  $W$  are all 20  $\mu\text{m}$ . In this figure, solid rectangles and open circles correspond to the data of the PGSS with a ground strip width  $T$  of 5  $\mu\text{m}$  and 20  $\mu\text{m}$ , respectively. As shown in Fig. 2, the wavelength of the coplanar waveguide was reduced to 60% to 65% of a conventional one by using PGSS. For example, the wavelength of the coplanar waveguide employing PGSS (with a  $T$  of 20  $\mu\text{m}$ ) is 3.7 mm at 20 GHz, while the wavelength of the conventional coplanar waveguide without PGSS is 5.9 mm at the same frequency.

The results indicate that highly miniaturized passive circuits can be realized by using a coplanar waveguide employing PGSS. Measured characteristic impedance of the coplanar waveguide employing PGSS is shown in Fig. 3, where  $W$  was fixed to a value of 20  $\mu\text{m}$ . The characteristic impedance of the coplanar waveguide  $Z_B$  was measured by the following method. Firstly, 50  $\Omega$ -based  $S$ -parameters of a coplanar waveguide were measured by network analyzer with 50  $\Omega$  port impedance. After this, the 50  $\Omega$ -based  $S$ -parameters were transformed to  $Z$ -parameters, and then, the  $Z$ -parameters were transformed to  $S$ -parameters for arbitrary port impedance  $Z_0$ [1]. If the arbitrary port impedance  $Z_0$  is the same as the characteristic impedance

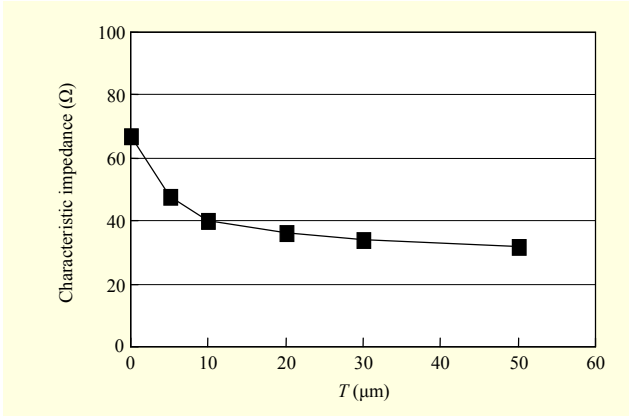


Fig. 3. Measured characteristic impedance of coplanar waveguide employing PGSS.

$Z_B$  of a coplanar waveguide, the return loss  $S'_{11}$  for the arbitrary port impedance becomes zero. Therefore,  $Z_B$  was obtained from the following condition,

$$|S'_{11}|_{Z_0=Z_B} = \left| \frac{(Z_{11} - Z_B)(Z_{22} + Z_B) - Z_{12}Z_{21}}{(Z_{11} + Z_B)(Z_{22} + Z_B) - Z_{12}Z_{21}} \right| = 0. \quad (2)$$

This process was automatically performed using a CAD tool.

In Fig. 3, as the  $T$  becomes larger, characteristic impedance becomes lower, because characteristic impedance is inversely proportional to a periodical capacitance of transmission line, in other words,  $Z_0 = [(R+L)/(G+C)]^{0.5}$ , and an increase of  $T$  results in an enhancement of periodical capacitance  $C_b$  due to an increase of capacitive area. For this reason, as shown in Fig. 3, characteristic impedance of the coplanar waveguide employing PGSS can be easily controlled simply changing the  $T$ . Especially, using PGSS, characteristic impedance can be reduced to a value much lower than a conventional coplanar waveguide. For example, as shown in Fig. 3, characteristic impedance shows a value of 67 Ω to 32 Ω by changing  $T$  from 0 μm to 50 μm. This characteristic is very favorable to a reduction of size of passive components on RFIC because a very low impedance line is required for impedance matching between active devices. In other words, the input/output impedance of FETs is much lower than 50 Ω (10 Ω to 40 Ω) in an RF band [4], and a very low impedance line should be used for impedance matching between FETs. For example, the  $W$  of a conventional coplanar waveguide (having a  $G$  of 30 μm) with a characteristic impedance of 35 Ω is 130 μm, while the  $W$  of a coplanar waveguide employing PGSS (having a  $T$  of 20 μm) with the same characteristic impedance is only 20 μm. Therefore, if a coplanar waveguide employing PGSS is used for impedance matching between active devices with low impedance,  $W$  can be highly reduced (by simply adjusting  $T$ ) compared with a conventional coplanar waveguide.

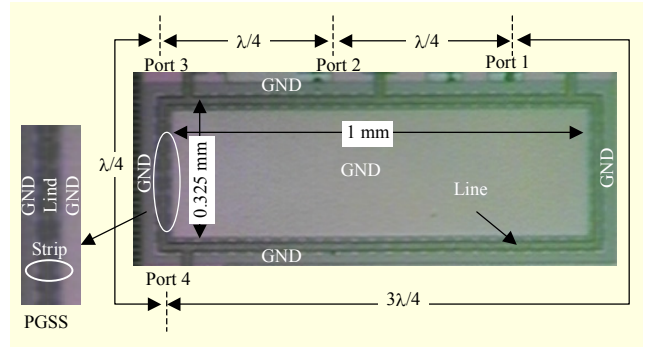


Fig. 4. Photograph of on-chip 180° hybrid employing PGSS on silicon substrate.

### III. RF Performances of the On-Chip 180° Hybrid Employing PGSS

Using the coplanar waveguide employing PGSS, a highly miniaturized on-chip 180° hybrid was developed for U-band RFIC applications.

Figure 4 shows a photograph of the on-chip 180° hybrid fabricated on a silicon substrate. Grand-signal-ground (GSG) pads were connected to input and output ports for on-wafer measurement. Because port impedance was set to 27 Ω for low impedance matching applications, the characteristic impedance of transmission lines comprising the 180° hybrid is 38 Ω. In order to realize the coplanar waveguide with 38 Ω, the value of  $T$  was set to 20 μm from Fig. 3. The length of the  $\lambda/4$  line comprising the 180° hybrid was determined from Fig. 2. In the case of a center frequency of 46 GHz, the size of the 180° hybrid employing PGSS was 0.325 mm<sup>2</sup>, which is 19.3% of the size of the one fabricated by a conventional coplanar waveguide [1]. In other words, in a case in which ring-shape 180° hybrid is fabricated by conventional coplanar waveguide (having a  $G$  of 30 μm) on a silicon substrate with a height of 600 μm, the length of the  $\lambda/4$  line is 0.718 mm at the center frequency, and the  $W$  of the coplanar waveguide with a characteristic impedance of 38 Ω is 90 μm. Therefore, the size of a ring-shaped 180° hybrid employing a conventional coplanar waveguide can be calculated as

$$\pi(3\lambda/4\pi + W/2)^2 = \pi(3 \times 2.872/4\pi + 0.09/2)^2 = 1.68 \text{ (mm}^2\text{)}.$$

In order to measure the insertion and return loss of the hybrid coupler, the GSG pattern should be used because the on-wafer measurement method is indispensable for a measurement of on-chip components on RFIC. Because the hybrid coupler is a 4 port device, unmeasured ports were terminated with a port impedance of 27 Ω, which was fabricated using a thin film resistor process on silicon substrate. When the port impedance is arbitrary, not 50 Ω, low impedance GSG probes with a port impedance of 27 Ω are required to obtain ideal measurement

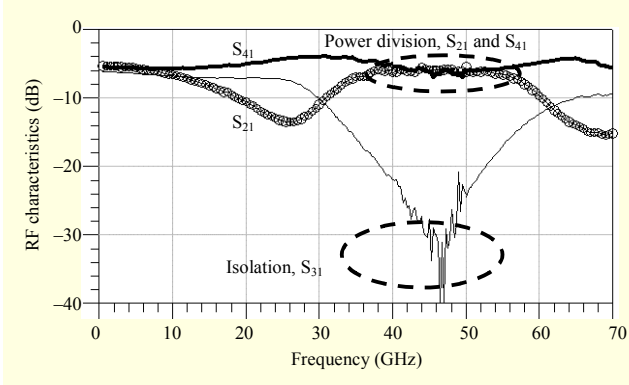


Fig. 5. Measured power division and isolation characteristics of the on-chip 180° hybrid employing PGSS.

result. However, there is no low impedance GSG probe for the on-wafer measurement method (all commercial GSG probes have a port impedance of 50 Ω). Therefore, in this work, 27 Ω-based  $S$ -parameters were obtained from measured 50 Ω-based  $S$ -parameters using well-known  $S$ -parameter transformation theory [1]. First, we measured 50 Ω-based  $S$ -parameters with a 50 Ω GSG probe, and then, the 50 Ω-based  $S$ -parameters were transformed into  $Z$ -parameters using

$$Z_{11} = 50 \frac{(1 + S_{11})(1 - S_{22}) + S_{12}S_{21}}{(1 - S_{11})(1 - S_{22}) - S_{12}S_{21}}, \quad (3)$$

$$Z_{12} = 50 \frac{2S_{12}}{(1 - S_{11})(1 - S_{22}) - S_{12}S_{21}}, \quad (4)$$

$$Z_{21} = 50 \frac{2S_{21}}{(1 - S_{11})(1 - S_{22}) - S_{12}S_{21}}, \quad (5)$$

$$Z_{22} = 50 \frac{(1 - S_{11})(1 + S_{22}) + S_{12}S_{21}}{(1 - S_{11})(1 - S_{22}) - S_{12}S_{21}}. \quad (6)$$

In (3) to (6),  $Z_{ij}$  and  $S_{ij}$  are  $Z$ -parameters and 50 Ω-based  $S$ -parameters, respectively. Finally, the  $Z$ -parameters were transformed into 27 Ω-based  $S$ -parameters using

$$S'_{11} = \frac{(Z_{11} - Z_0)(Z_{22} + Z_0) - Z_{12}Z_{21}}{\Delta Z}, \quad (7)$$

$$S'_{12} = \frac{2Z_{12}Z_0}{\Delta Z}, \quad (8)$$

$$S'_{21} = \frac{2Z_{21}Z_0}{\Delta Z}, \quad (9)$$

$$S'_{22} = \frac{(Z_{11} + Z_0)(Z_{22} - Z_0) - Z_{12}Z_{21}}{\Delta Z}, \quad (10)$$

$$|\Delta Z| = (Z_{11} + Z_0)(Z_{22} + Z_0) - Z_{12}Z_{21}. \quad (11)$$

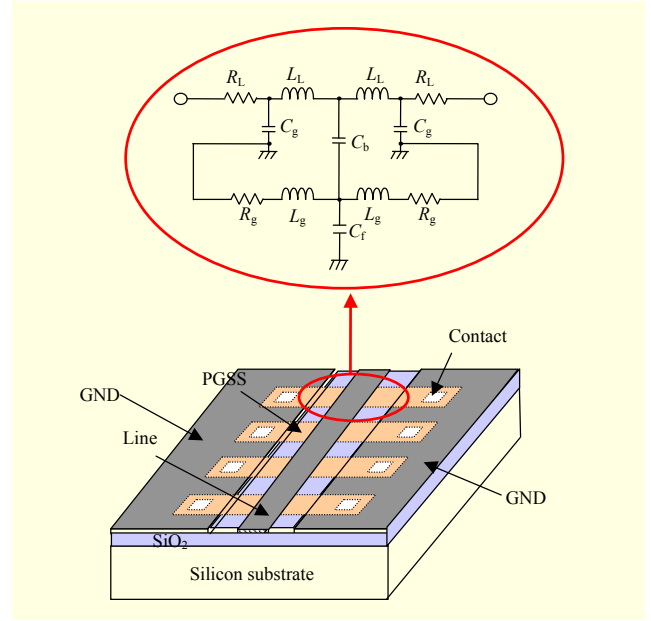


Fig. 6. Structure of the coplanar waveguide employing PGSS.

In (7) to (11),  $S'_{ij}$  are 27 Ω-based  $S$ -parameters, and  $Z_0$  is 27 Ω. To perform an accurate measurement, we extracted the PAD capacitance using the  $Y$ -parameter de-embedding method [10]. Figure 5 shows the power division and isolation characteristics of the 180° hybrid employing PGSS. We can observe good power division characteristics from 37 GHz to 55 GHz. Concretely,  $S_{21}$  and  $S_{41}$  exhibit a value of  $-5.5$  dB at 46 GHz. In a frequency range of 37 GHz to 55 GHz,  $S_{21}$  and  $S_{41}$  both show a value of  $-5.5 \pm 0.5$  dB. Actually, a value of power division of the 180° hybrid fabricated on teflon substrate [1] is about  $-5 \pm 0.5$  dB, and the 180° hybrid employing PGSS shows a loss higher by 0.5 dB over a conventional 180° hybrid which originated from high conductivity of a silicon substrate. To investigate the loss characteristic of the coplanar waveguide employing PGSS, we evaluated the inductive quality factor using

$$Q_L = \frac{\omega L_L}{R_L}. \quad (12)$$

To evaluate inductive quality factor  $Q_L$ , the series resistance  $R_L$  and inductance  $L_L$  should be obtained from the coplanar waveguide employing PGSS. For this reason, we extracted the equivalent circuit of the coplanar waveguide employing PGSS. Figure 6 shows the structure of the coplanar waveguide employing PGSS and its equivalent circuit of single cell. Using the equivalent circuit, the inductive quality factor  $Q_L$  was evaluated. According to the results, the coplanar waveguide employing PGSS showed  $Q_L$  values higher than 10 at 50 GHz in a range of  $T$  from 5 μm to 20 μm. At this time, the accuracy of the  $Q_L$  values was not guaranteed because it is very difficult

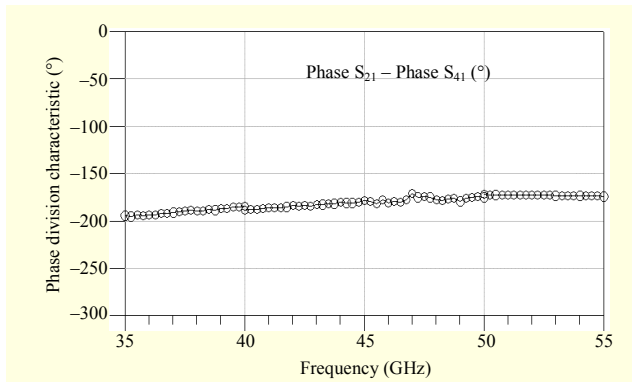


Fig. 7. Measured phase division characteristic of the on-chip 180° hybrid employing PGSS.

to obtain an accurate equivalent circuit of the coplanar waveguide employing PGSS due to its complicated structure. Therefore, we have to study an accurate equivalent circuit to obtain more accurate values of  $Q_L$ .

The isolation characteristic  $S_{31}$  shows a value of  $-40$  dB at 46 GHz, and values better than  $-18.5$  dB in a frequency range of 37 GHz to 55 GHz. Figure 7 shows the phase division characteristic of the 180° hybrid employing PGSS. The phase division shows a value of  $180.3^\circ$  at 46 GHz and values of  $180^\circ \pm 4.9^\circ$  in a frequency range of 37 GHz to 55 GHz.

#### IV. Conclusion

We fabricated a highly miniaturized on-chip 180° hybrid employing PGSS on a silicon substrate for U-band RFIC applications. The PGSS was placed at the interface between  $\text{SiO}_2$  film and a silicon substrate, and it was electrically connected to top-side GND planes through the contacts. Owing to the short wavelength characteristic of the transmission line employing the PGSS, an on-chip 180° hybrid was highly miniaturized on the silicon substrate. According to measured results, the 180° hybrid showed good RF performances from 37 GHz to 55 GHz, and its size was  $0.325 \text{ mm}^2$ , which was 19.3% of the size of one fabricated by a conventional coplanar waveguide.

#### References

- [1] D.M. Pozar, *Microwave Engineering*, Reading, MA: Addison-Wesley, 1990.
- [2] M. Chongcheawchamnam, N. Siripon, and I.D. Robertson, "Design and Performance of Improved Lumped-Distributed Wilkinson Divider Topology," *Electron. Lett.*, vol. 37, no. 8, Apr. 2001, pp. 501-503.
- [3] D.R. Webster, G. Ataei, and D.G. Haigh, "Low-Distortion MMIC Power Amplifier Using a New Form of Derivative

- Superposition," *IEEE Trans. Microw. Theory Tech.*, vol. 49, no. 2, Feb. 2001, pp. 328-332.
- [4] Y. Yun et al., "A High Performance Downconverter MMIC for DBS Applications," *IEICE Trans. Electron.*, vol. E84-C, no. 11, Nov. 2001, pp. 1679-1688.
- [5] M. Zargari and D. Su, "Challenges in Designing CMOS Wireless Systems-on-a-Chip," *IEICE Trans. Electron.*, vol. E90-C, no. 6, Jun. 2007, pp. 1142-1148.
- [6] Y. Yun et al., "Experimental Study on Isolation Characteristics Between Adjacent Microstrip Lines Employing Periodically Perforated Ground Metal for Application to Highly Integrated GaAs MMICs," *IEEE Microw. Wireless Compon. Lett.*, vol. 17, no. 10, Oct. 2007, pp. 703-705.
- [7] S. Seki and H. Hasegawa, "Cross-Tie Slow-Wave coplanar Waveguide on Semi-Insulating GaAs Substrate," *Electron. Lett.*, vol. 17, no. 25, Dec. 1981, pp. 940-941.
- [8] T.S.D. Cheung and J.R. Long, "Shielded Passive Devices for Silicon-Based Monolithic Microwave and Millimeter-Wave Integrated Circuits," *IEEE J. Solid-State Circuits*, vol. 41, no. 5, May 2006, pp. 1183-1200.
- [9] Y. Yun et al., "Miniaturized On-Chip Branch-line Coupler Employing Periodically Arrayed Grounded-Strip Structure for Application to Silicon RFIC," *Microw. J.*, vol. 52, no. 12, 2009, pp. 90-98.
- [10] P.J. van Wijnen, H.R. Claessen, and E.A. Wolsheimer, "A New Straightforward Calibration and Correction Procedure for On Wafer High Frequency S-Parameter Measurements," *IEEE BCTM*, 1987, pp. 70-73.



**Young Yun** received the BS in electronic engineering from Yonsei University, Seoul, Korea, in 1993, the MS in electrical and electronic engineering from Pohang University of Science and Technology, Pohang, Korea, in 1995, and the PhD in electrical engineering from Osaka University, Osaka, Japan, in 1999.

From 1999 to 2003, he worked as an engineer in Matsushita Electric Industrial Company Ltd. (Panasonic), Osaka, Japan, where he was engaged in the research and development of monolithic microwave ICs (MMICs) for wireless communications. In 2003, he joined the Department of Radio Communication Engineering, Korea Maritime University, Busan, Korea, where he is currently an associate professor. Since 2008, he has served as an associate editor of the Institute of Electronics, Information and Communication Engineers (IEICE) in Japan, and as an editor of the Korean Society of Marine Engineering in Korea. He is the author and co-author of over 100 international journals and 15 patents pending in RF/microwave device and IC. His research interests include design and measurement for RF/microwave and millimeter-wave ICs, and design and fabrication for HEMT and HBT.